DOI: 10.1002/pul2.12412

RESEARCH ARTICLE

Pulmonary Circulation Open Access | PVRI | WILEY

Nanoparticle delivery of VEGF and SDF-1α as an approach for treatment of pulmonary arterial hypertension

Victoria A. Guarino | **Bradley M. Wertheim** | **Wusheng Xiao** | **Joseph Loscalzo** | **Ying-Yi Zhang**

Harvard Medical School, Brigham and Women's Hospital, Boston, Massachusetts, USA

Correspondence
Joseph Loscalzo, Brigham and Women's Hospital, Harvard Medical School, 77 Ave Louis Pasteur, NRB 630, Boston, MA 02115, USA.
Email: jloscalzo@bwh.harvard.edu

Funding information
Astellas Institute for Regenerative Medicine

Abstract

Endothelial dysfunction is an underlying mechanism for the development of pulmonary arterial hypertension (PAH). Vascular endothelial growth factor (VEGF) and stromal cell-derived factor-1α (SDF) may help repair the dysfunctional endothelium and provide treatment for PAH. To examine this possibility, nanoparticles carrying human recombinant VEGF and SDF (VEGFNP and SDFNP) were aerosolized into the lungs of nude rats at Day 14 after monocrotaline (MCT) injection and analyses were performed at Day 28. The data show that the VEGFNP/SDFNP delivery led to a lower pulmonary arterial pressure and prevented right ventricular hypertrophy in the MCT rats: the right ventricular systolic pressure of the control, MCT, and MCT + VEGFNP/SDFNP treatment groups were 29±2, 70±9, and 44±5 (mean±SD) mmHg, respectively; the pulmonary vascular resistance indices of the groups were 0.6±0.3, 3.2±0.7, and 1.7±0.5, respectively; and the Fulton indices [−RV/(LV + Septum)] were 0.22±0.01, 0.44±0.07, and 0.23±0.02, respectively. The VEGFNP/SDFNP delivery delayed the thickening of distal pulmonary vessels: the number of nearly occluded vessels in a whole lung section from the MCT and MCT + VEGFNP/SDFNP groups were 46±12 and 2±3, respectively. Gene expression analysis of the endothelial cell markers, VE-cadherin, KDR, BMPR2, and eNOS, and smooth cell markers, SM-MHC and α-SMA, indicated significant loss of distal pulmonary vessels in the MCT- treated rats. VEGFNP/SDFNP delivery did not recover the loss, but significantly increased eNOS and decreased α-SMA expression in the MCT-treated lungs. Thus, the therapeutic effect of VEGFNP/SDFNP may be mediated by improving/repairing endothelial function in the PAH lungs.

KEYWORDS
eNOS, monocrotaline, nanoparticle delivery, therapeutic

INTRODUCTION

Vascular endothelial growth factor (VEGF) plays an important role in maintenance and repair of adult endothelium. As such, it may be useful for the treatment of pulmonary arterial hypertension (PAH) since endothelial injury and dysfunction is an underlying mechanism for the development of PAH.[1]

The effect of VEGF in PAH has been previously investigated: delivery of VEGF to the lungs of hypoxic rats by adenovirus-mediated gene transfer showed a protective effect against PAH.[2] Blocking VEGF signaling by inhibition of its receptor (VEGFR2/KDR/flk-1) with SU5416 markedly exacerbated PAH in chronic hypoxic rats and mice.[3,4] Knockout of the endothelial VEGF receptor gene in mice produced similar effects as that of SU5416.[5,6] Some patients with heritable PAH were found to carry heterozygous loss-of-function mutations in the KDR gene.[7] Ex vivo CT angiography of barium-injected lungs in SU5416-treated hypoxic mice showed significant pruning of peripheral pulmonary vessels compared with those in vehicle-treated hypoxic mice.[4] Taken together, these results show that VEGF has a protective effect against the development of severe PAH.

While PAH patients exhibit pruning of peripheral pulmonary vessels, exuberant endothelial cell growth was found in their plexiform lesions.[8] Monoclonal expansion of endothelial cells was observed in plexiform lesions of primary and appetite suppressant-associated PAH.[9,10] These phenomena point to the possibility that some of the resident endothelial progenitor cells in the PAH lungs may have been compromised by the insult that initially caused PAH and gained different growth characteristics. Maintaining or proliferating these types of cells by VEGF would be futile or even harmful in terms of treatment of PAH. Injury or transformation of lung resident endothelial progenitor cells could also occur in animal models of PAH. SDF-1α (SDF) is known to play important roles in mobilization, recruitment, retention, and differentiation of bone marrow-derived progenitor cells in tissue.[11–13] For this reason, we delivered SDF together with VEGF in the present study to facilitate utilizing extra-pulmonary progenitor cells for pulmonary endothelial repair.

To deliver VEGF and SDF effectively to the lung, nanoparticle incorporation of the proteins is required. Since VEGF is also a vascular permeability factor (VPF) [14] and SDF is a potent chemokine, only a small amount of these proteins can be safely delivered to the lung without causing pulmonary edema,[15] hemorrhage, or inflammation. Yet, clearance of the delivered proteins in the lung is very rapid (in hours), which could reduce the concentration of the delivered proteins below their EC_{50}s before biological effects take place. To extend the retention time of the delivered proteins in the lung, this study used a crosslinked dextran sulfate chitosan nanoparticle (XNP) as a carrier for protein delivery. Our previous study showed that by incorporation into XNP, the time for 50%, 90%, and 99% clearance of SDF in the lung increased from 2, 6, and 12 h to 1.3, 4.4, and 8.7 days, respectively.[16] After 99% clearance, the concentration of XNP-incorporated SDF in the lung was estimated to be near its EC_{50}.

To study the effect of these human proteins in rat lungs, immune-suppressed or -deficient rats were found to be necessary. In our initial studies, the nanoparticle-incorporated human VEGF and SDF showed no effect in monocrotaline (MCT)-induced PAH in wildtype Sprague Dawley rats, but had some preventive effect in cyclosporine A (CsA)-treated Sprague Dawley rats (see Section 3). These results suggested that immune elimination of the nanoparticle-delivered human proteins (and/or a possible inflammatory response) had likely occurred in the wildtype Sprague Dawley rats. Considering that the CsA treatment does not completely block the immune system, athymic nude rats were used in the next phase of the study to investigate the therapeutic effect of VEGF and SDF in MCT-induced PAH. A diagram of the experimental design is shown in Figure 1.

METHODS

Preparation of nanoparticles

Nanoparticles were prepared in three stages, which produced dextran sulfate-chitosan nanoparticles (DSCS NPs), crosslinked DSCS NPs (XNPs), and VEGF- or SDF-incorporated XNP (VEGFNP or SDFNP) consecutively. The detailed procedures for the DSCS NP and XNP preparations have been previously described.[16,17] For the VEGFNP or SDFNP preparation, the amount of charged dextran sulfate on the surface of XNPs was first determined with an Azure A assay[17] and used to quantify the amount of XNP. The XNPs were diluted in a sterile glass bottle with phosphate-buffered saline (PBS) to a concentration of approximately 0.1 mg/mL and stirred at 700 rpm. The amount of the VEGF or SDF to be incorporated into the XNPs was calculated according to a protein-to-particle ratio of 0.3 mg/mg for SDF or 0.5 mg/mg for VEGF. VEGF or SDF was then diluted to 0.1–0.15 mg/mL in PBS, and added slowly to the stirring XNPs at approximately 0.2 mL/min. The mixture was stirred for an additional 25 min at 500 rpm, and the formed VEGFNPs or SDFNPs were precipitated by centrifugation at 20,000*g* for 15 min. The particles were suspended in 5%

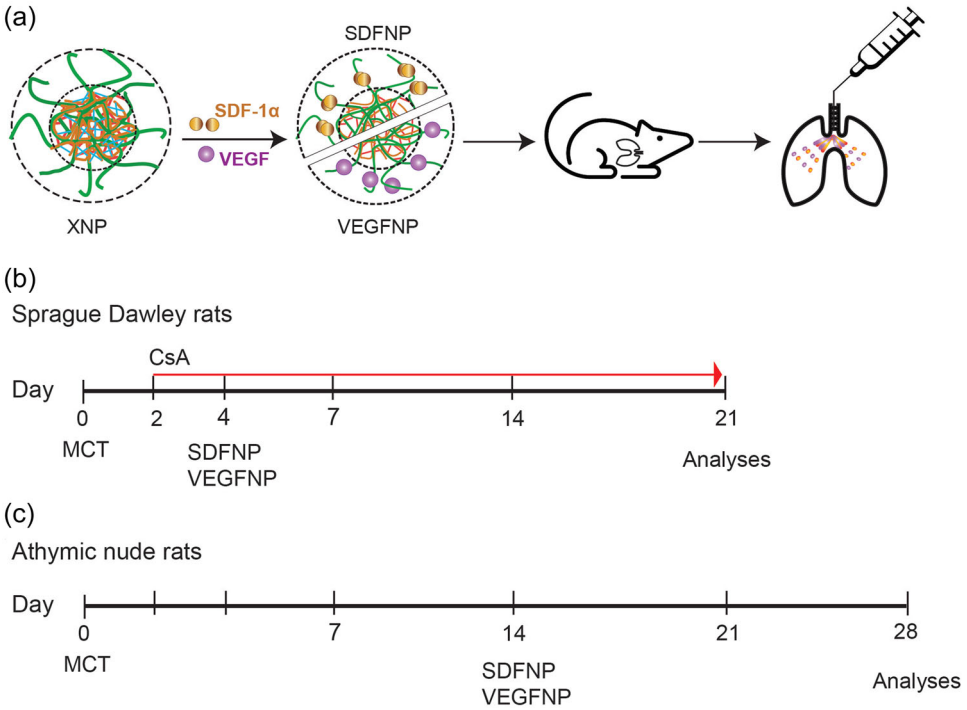

FIGURE 1 Schematic of the experimental design. Crosslinked dextran sulfate chitosan nanoparticles (XNP) were prepared and loaded with recombinant human vascular endothelial growth factor (VEGF) or stromal cell-derived factor-1α (SDF) to produce VEGFNP or SDFNP, respectively. The particles were delivered to the lungs of rats by intratracheal aerosolization (a). Effects of the particles in pulmonary arterial hypertension (PAH) were examined in a rat monocrotaline (MCT) model using cyclosporine (CsA)-treated Sprague Dawley rats (b) or athymic nude rats (c). The treatment time course and particle delivery time are shown in the diagram.

mannitol, divided into small aliquots, and stored frozen until application. The exact amounts of the proteins in the particles were determined by sodium dodecyl sulfate-polyacrylamide gel electrophoresis (for details, see Guarino et al.[16]). The particle diameter, polydispersity index, and zeta potential were measured by dynamic light scattering using a Zetasizer instrument (Malvern Instruments) according to the manufacturer's instructions.

Animal treatment

All animal experiments were approved by the Brigham and Women's Hospital Institutional Animal Care and Use Committee. Male Sprague Dawley rats (200–225 g) and homozygous athymic nude rats (8-week-old) were obtained from Charles River Laboratories and were acclimated for 6–9 days under standard conditions following US National Institutes of Health guidelines. Nude rats were housed in a sterile environment. Sprague Dawley rats received CsA at 10 mg/kg/day by subcutaneous injection of Sandimmune (Days 2–10) and by drinking Neoral oral solution diluted in 1.6% sucrose/water (Days 11–21). MCT (Oakwood Products Inc. # 002602, Lot 002602J08E) was injected intraperitoneally to the rats on day 0 at a single dose of 55 mg/kg for Sprague Dawley rats and 50 mg/kg for nude rats. VEGFNP and SDFNP were delivered (see below) to the CsA-treated Sprague Dawley rats at Day 4 and to nude rats at Day 14 after MCT injection. Hemodynamic analysis and tissue harvest were performed at the end of the study, which were Day 21 for the CsA Sprague Dawley rats and Day 28 for the nude rats. The time course for each type of rat had been previously tested and selected, in which the right ventricular systolic pressure peaked at the end of the studies and right heart failure became apparent the week thereafter.

Nanoparticle delivery

Nanoparticles containing 8 μg VEGF (VEGFNP) and 4 μg SDF (SDFNP) were diluted together in Dulbecco's PBS to a final volume of 0.25 mL and aerosolized into rat lungs as following: Rats were anesthetized with ketamine/xylazine and placed on a Tilting WorkStand (Hallowell EMC). The vocal cords of the animal were visualized with a specula-attached otoscope. A small amount (2–5 μL) of 2% lidocaine HCl jelly was applied to the vocal cords and surrounding vestibular folds. The respiration of the rat was monitored. A sterilized

MicroSprayer Aerosolizer (Model IA-1B-R was obtained from Penn-Century, Inc.) attached to a 0.5 mL gas-tight syringe was inserted into the trachea and advanced to approximately 1 cm above the bifurcation point. At a respiratory rate of approximately 70–90 BPM, 0.25 mL nanoparticle suspension, behind which was a 0.2 mL column of air was aerosolized into the lung. After aerosolization, rats were placed on a warm pad to recover before returning to their cages.

Hemodynamic analysis and tissue harvest

Hemodynamic analyses were performed to determine the right ventricular systolic pressure (RVSP) and pulmonary vascular resistance (PVR). To measure the right ventricular (RV) pressure, a J-shaped PE-50 tubing catheter was inserted into the right ventricle through the right jugular vein following the pressure waveform. The catheter was connected to a Deltran® disposable blood pressure transducer (Utah Medical Products) which sent the pressure signal through a Bridge Amplifier to a Powerlab 8/35 instrument (ADInstruments). The recorded signals were measured and analyzed with LabChart 8 software. The reported RVSP was an average of measurements of max-min pressure from 200 to 400 consecutive cardiac cycles (~1 min tracing after signal stabilized). The left ventricular (LV) hemodynamic parameters were measured with a Mikro-Tip® rat pressure-volume catheter (Millar, #SPR-869), which was inserted into the left ventricle through the right carotid artery. The catheter was connected to a MPVS Ultra Pressure-Volume Unit (Millar) which sent the signals of pressure and relative volume to the Powerlab 8/35 for measurement and analysis. The reported pulmonary vascular resistance (PVR) was calculated as (RV mean pressure − LV end diastolic pressure)/cardiac output (mmHg*min/mL) and was an average of measurements from 50 to 200 consecutive cardiac cycles. PVR index was calculated as PVR/body weight (mmHg*min/mL/kg). After the hemodynamic analysis, the heart and lungs were perfused with PBS through the pulmonary artery. The weight ratio of RV-to-(LV + septum) [RV/(LV + S)] (Fulton index) was measured. The right lung was dissected, frozen in liquid nitrogen, and stored at −80°C. The left lung was inflated with 10% phosphate-buffered formalin at 20 cm H_2O pressure and fixed for 24 h before tissue processing.

Histological analysis

The formalin-fixed left lung was divided into four transverse segments. The segments were processed, paraffin embedded, and cut into 5 μm tissue sections. Hematoxylin and eosin (H&E) staining was performed. Muscularized distal vessels were counted throughout the whole section from the third segment (from the top) of the lung.

Gene expression analysis

The whole right lung of rats was homogenized by cryo-grinding using a bead beater, Spex 1600 miniG homogenizer. The resulting tissue powder was stored at −80°C, and aliquots were used for RNA isolation. RNA was prepared by extraction of the tissue powder with TRIzol Reagent and then purified with a RNeasy Plus Mini kit (Qiagen) following the manufacturer's instructions. cDNA was synthesized using a High-Capacity cDNA Reverse Transcription Kit (Applied Biosystems). Gene expression analysis was performed with a TaqMan Real-time polymerase chain reaction (RT-PCR) assay using an RT-PCR System (Applied Biosystems), TaqMan probes/primers, and TaqMan Universal Master Mix provided by the manufacturer.

Statistics

Statistical analyses were performed by one-way analysis of variance and Tukey's multiple comparison using Prism software (GraphPad). Data are presented as mean ± standard deviation. *p*-Values are denoted as follows: ns, $p > 0.05$; *$p \le 0.05$; **$p \le 0.01$; ***$p \le 0.001$; and ****$p \le 0.0001$.

RESULTS

In vitro characteristics of VEGFNP and SDFNP

To extend the retention time of VEGF and SDF in the lung, the proteins were incorporated into nanoparticles, XNPs, to form VEGFNP and SDFNP (for details, see Section 2). The prepared VEGFNP and SDFNP had similar physical and biological properties as we previously reported[16]: the sizes of the particles were 300–350 nm, Zeta potentials were −42 to −44 mV, and the polydispersity index were 0.05–0.1. VEGFNP had the same activity as VEGF in proliferation assays of human pulmonary artery endothelial cells. SDFNP had the same activity as SDF in Jurkat cell migration assays. The incorporated VEGF or SDF were not released from the particles for at least 14 days when incubated at 37°C, and their activities were fully maintained during this time (for analysis procedures of these properties, see Guarino et al.[16]).

Preventive effects of VEGFNP/SDFNP

To examine the effect of VEGFNP/SDFNP in PAH, a preventive treatment with the particles was carried out in CsA-treated Sprague Dawley rats. VEGFNP (8 μg) and SDFNP (4 μg) were aerosolized together into the lungs of the rats at Day 4 after MCT injection, and hemodynamic analysis was carried out at Day 21. Pilot studies had shown that the pulmonary arterial pressure in this model peaked at 3 weeks after MCT injection (55 mg/kg, IP), which was followed by right heart failure in about a week.

As shown in Figure 2, the VEGFNP/SDFNP delivery significantly reduced the right ventricular systolic pressure (RVSP) and the pulmonary vascular resistance (PVR) in the MCT-treated rats: the RVSP of the Ctrl, MCT, and MCT plus VEGFNP/SDFNP groups were 31±1.5, 81±4.8, and 54±4.3 mmHg, respectively (Figure 2a); the PVR indices of the groups were

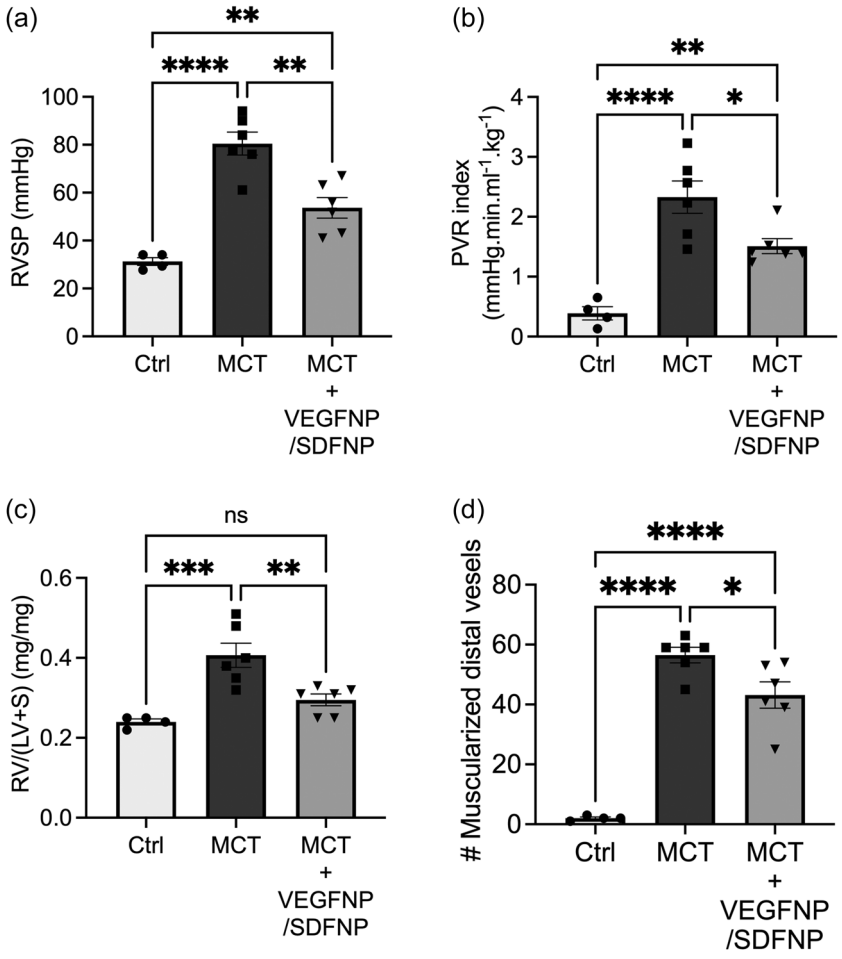

FIGURE 2 Preventive effect of VEGFNP/SDFNP in development of PAH. VEGFNP/SDFNP were aerosolized into CsA-treated Sprague Dawley rats at Day 4 after MCT injection. Measurements were performed at Day 21 in rats treated with nothing (Ctrl), MCT, or MCT + VEGFNP/SDFNP. (a) right ventricular systolic pressure (RVSP), (b) pulmonary vascular resistance index (PVR index), (c) weight ratio of right ventricle-to-(left ventricle + septum) [RV/(LV + S)], and (d) total number of muscularized distal pulmonary vessels. ns, $p > 0.05$; *$p \leq 0.05$; **$p \leq 0.01$; ***$p \leq 0.001$; and ****$p \leq 0.0001$. MCT, monocrotaline; NP, nanoparticles; PAH, pulmonary arterial hypertension; SDF, stromal cell-derived factor-1α; VEGF, vascular endothelial growth factor.

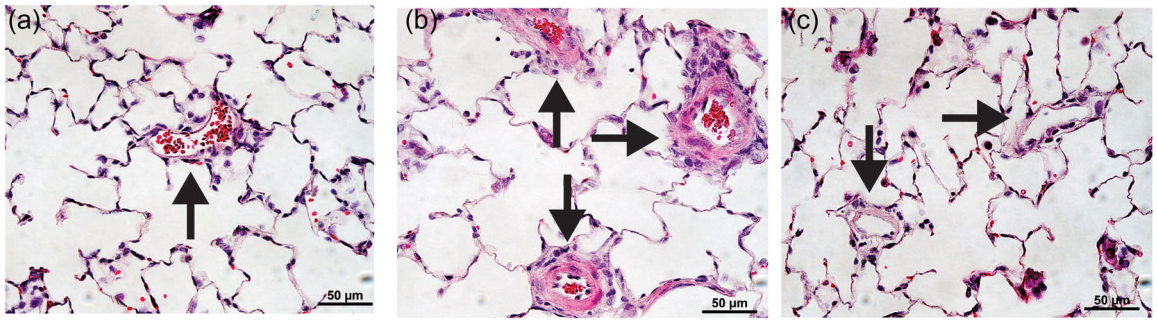

FIGURE 3 H&E-stained lung tissue sections from the preventive study. Lung sections were from CsA-Sprague Dawley rats treated with (a) nothing (Ctrl), (b) MCT, and (c) MCT + VEGFNP/SDFNP. H&E, hematoxylin and eosin; MCT, monocrotaline; NP, nanoparticles; SDF, stromal cell-derived factor-1α; VEGF, vascular endothelial growth factor.

0.39±0.11, 2.33±0.27, and 1.51±0.13 mmHg/mL/min, respectively (Figure 2b). VEGFNP/SDFNP prevented right ventricular hypertrophy in the MCT treated rats. The weight ratios of the right ventricle-to-(left ventricle + septum) [RV/(LV + S)] (Fulton Index) of the Ctrl, MCT, and MCT plus VEGFNP/SDFNP groups were 0.24±0.01, 0.41±0.03, and 0.30±0.02, respectively (Figure 2c). There was no statistical difference between the Ctrl and the VEGFNP/SDFNP treated groups.

Histological analysis of the lung tissue sections showed that MCT treatment caused significant medial thickening of distal pulmonary vessels in the rats (Figure 3b), which was reduced with VEGFNP/SDFNP treatment (Figure 3c). However, there were significant numbers of initially muscularized, thin-walled distal vessels in the VEGFNP/SDFNP-treated lungs. The total number of muscularized distal vessels in the Ctrl, MCT, and MCT + VEGFNP/SDFNP groups were 2±0.4, 57±2.6, and 43±4.4, respectively (Figure 2d).

Therapeutic effects of VEGFNP/SDFNP

Nude rats were used to evaluate the therapeutic effect of VEGFNP/SDFNP in the MCT model of PAH. Pilot studies had shown that the increase in pulmonary arterial pressure in the nude rat model peaked at about 4 weeks after MCT injection (50 mg/kg, IP). In this study, VEGFNP/SDFNP was delivered to MCT-injected nude rats at Day 14, and hemodynamic analysis was carried out at Day 28. Five treatment groups were examined: Ctrl, MCT only, MCT plus 8 μg VEGFNP and 4 μg SDFNP (MCT + VEGFNP/SDFNP), MCT plus 8 μg VEGF and 4 μg SDF (MCT + VEGF/SDF), and MCT plus empty nanoparticle (MCT + XNP).

As shown in Figure 4, VEGFNP/SDFNP significantly reduced the pulmonary arterial pressure and pulmonary vascular resistance in the MCT rats. The RVSPs of the Ctrl, MCT, and MCT + VEGFNP/SDFNP groups were 29±2, 70±9, and 44±5 mmHg, respectively (Figure 4a), and the PVR indices of the groups were 0.6±0.3, 3.2±0.7, and 1.7±0.5, respectively (Figure 4b). VEGFNP/SDFNP treatment prevented right ventricular hypertrophy in the MCT injected rats: the RV/(LV + S) ratio of the Ctrl, MCT, and MCT + VEGFNP/SDFNP groups were 0.22±0.01, 0.44±0.07, and 0.23±0.02, respectively (Figure 4c). The VEGF/SDF group and the XNP group did not show differences in the RVSP, PVR index, and RV/(LV + S) compared with the MCT group (Figure 4a–c), indicating that nanoparticle incorporation is necessary for the therapeutic effects of VEGF and SDF.

Histological analysis was carried out in the H&E-stained left lung sections of rats. The lung sections from

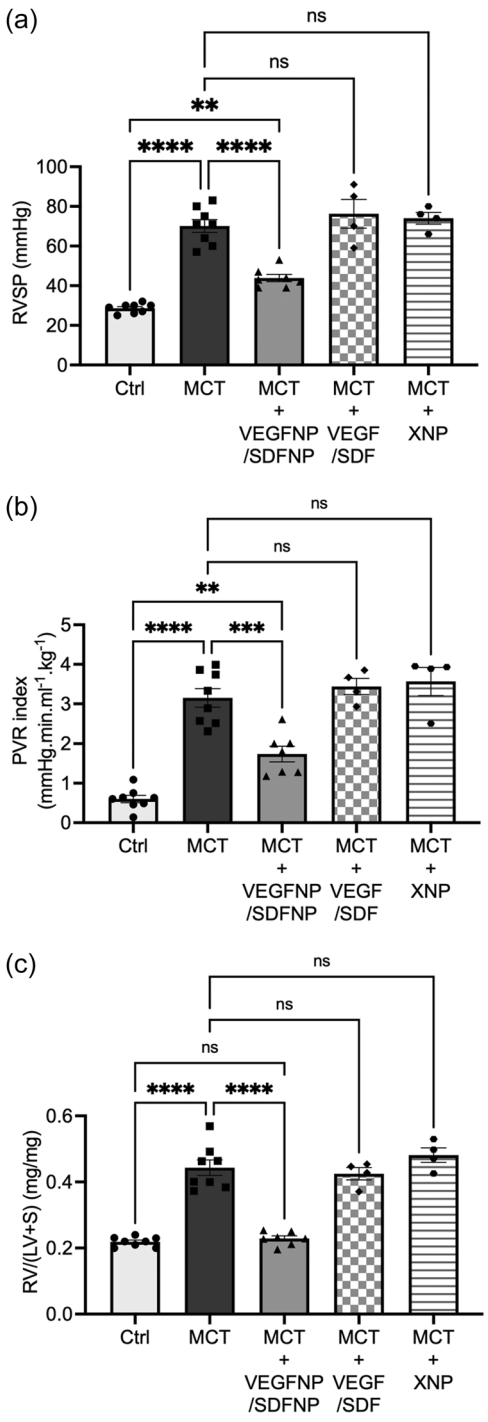

FIGURE 4 Therapeutic effect of VEGFNP and SDFNP in the development of PAH. VEGFNP/SDFNP were aerosolized into the lungs of nude rats at Day 14 after MCT injection. Measurements were performed at Day 28 in rats treated with nothing (Ctrl), MCT, MCT + VEGFNP/SDFNP, MCT + VEGF/SDF or MCT + XNP. (a) RVSP, (b) PVR index, (c) Weight ratio of right ventricle to left ventricle plus septum [RV/(LV + S)]. ns, $p > 0.05$; ** $p \le 0.01$; *** $p \le 0.001$; and **** $p \le 0.0001$. MCT, monocrotaline; NP, nanoparticles; PAH, pulmonary arterial hypertension; PVR, pulmonary vascular resistance; SDF, stromal cell-derived factor-1α; VEGF, vascular endothelial growth factor.

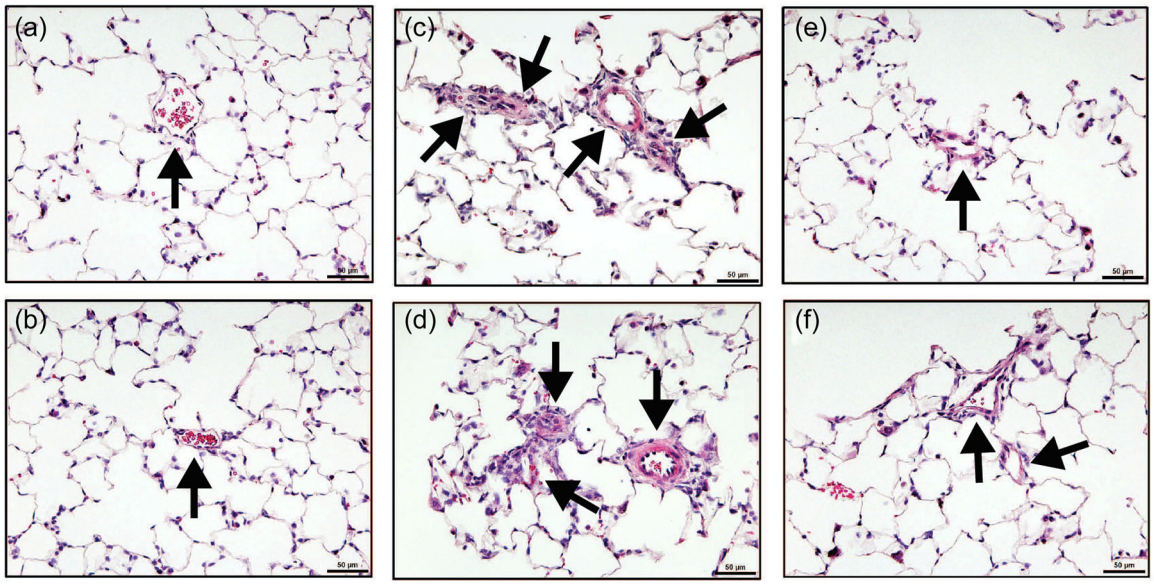

FIGURE 5 H&E-stained lung tissue sections from the therapeutic study. Lung sections were from nude rats treated with (a and b) nothing (Ctrl), (c and d) MCT, or (e and f) MCT + VEGFNP/SDFNP. H&E, hematoxylin and eosin; MCT, monocrotaline; NP, nanoparticles; SDF, stromal cell-derived factor-1α; VEGF, vascular endothelial growth factor.

all groups appeared "clean" with minimal macrophage infiltration or inflammation. However, muscularization and medial thickening of distal pulmonary vessels was prominent in the MCT-treated lungs. The micro images of the lung sections are shown in Figure 5.

The numbers of muscularized distal vessels were counted according to their wall thickness throughout the whole lung sections. The vessel wall thickness was expressed as % medial thickness, which was estimated as a percentage of (external diameter – internal diameter)/external diameter of the vessel wall. The muscularized distal vessels were counted in three groups with medial thicknesses of 5%–20%, 25%–75%, and 80%–100%, representing initially muscularized, thickened, and near occluded distal vessels, respectively. Examples of the groups are shown in Figure 6a, and the data are plotted in Figure 6b. There was a shift in the medial thickness pattern between the MCT and MCT + VEGFNP/SDFNP groups. While the MCT + VEGFNP/SDFNP group had more 5%–20% thickened vessels than that of the MCT group (64±12 vs. 24±7), it had significantly less 25%–75% thickened vessels (39±11 vs. 88±5) and minimal 80%–100% thickened vessels compared to the MCT group (2±3 vs. 46±12). Considering the Ctrl lungs had barely any muscularized distal vessels, the shift indicated that the VEGFNP/SDFNP prevented the progression of vascular thickening from initial muscularization to near occlusion of the vessel lumen. The total number of muscularized distal vessels are plotted in Figure 6c, which are 3±1, 158±12, and 106±23 in the Ctrl, MCT, and MCT + VEGFNP/SDFNP groups, respectively.

Endothelial and smooth muscle cells markers

Expression of endothelial cell and smooth muscle cell markers in the lung were examined with the samples from the nude rat study. Tissue homogenates were prepared from the whole right lungs of the rats. Aliquots of the homogenate were used for RNA extraction and PCR quantification.

As shown in Figure 7, expression of VE-Cadherin, KDR, and BMPR2 were significantly lower in the MCT lungs compared to that of Ctrl. As VE-cadherin is a structural protein and is constitutively expressed, the reduced RNA message of this marker indicates a loss of endothelial cells in the lungs of MCT-treated rats. This finding is consistent with a previous imaging study showing significant pruning of distal pulmonary vessels in the lungs of MCT-treated Sprague Dawley rats.[18] VEGFNP/SDFNP delivery did not change the reduced expression of VE-cadherin, indicating that a recovery of the lost endothelial cells via angiogenesis did not occur with the treatment. Expression of eNOS (Figure 7d) was different from that of the structural/receptor endothelial cell markers, which was comparable between the MCT and the Ctrl group. Considering the loss of endothelial cells in the MCT-treated lungs, the similar level of eNOS message in the Ctrl and MCT groups suggests a relative increase in eNOS expression in the MCT lungs. This phenomenon has been previously reported in the lungs of MCT-treated Sprague Dawley rats.[19] VEGFNP/SDFNP delivery

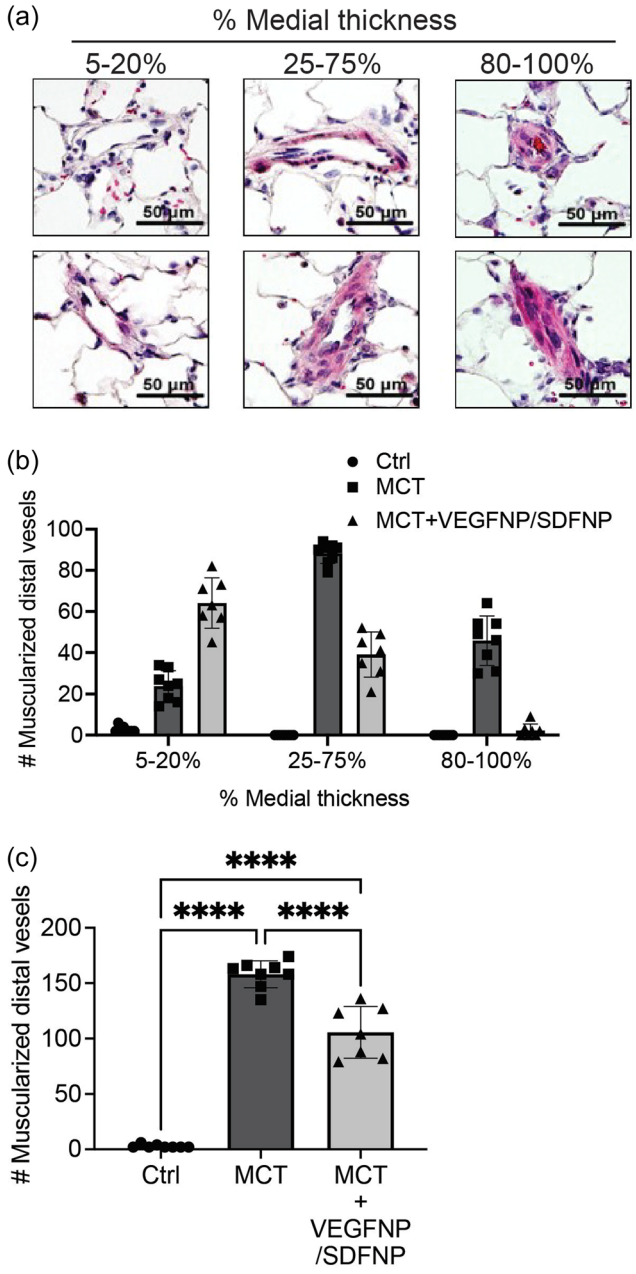

FIGURE 6 Number of thickened distal pulmonary vessels. (a) Muscularized distal pulmonary vessels were grouped according to % medial thickness, which was estimated as the percentage, (external diameter – internal diameter)/external diameter of the vessel wall X 100. (b) Number of muscularized distal vessels counted according to their medial thickness in a whole lung section of nude rats. (c) Total number of muscularized distal vessels in a whole lung section. ****$p \leq 0.0001$.

enhanced eNOS expression further in the MCT-treated rats, which was likely mediated by VEGF function (see discussion) and is in line with the beneficial effect of VEGFNP/SDFNP in PAH.

Expression of smooth muscle cell markers, smooth muscle-myosin heavy chain (SM-MHC) and α-smooth muscle actin (α-SMA), was also examined. As shown in Figure 7e, expression of SM-MHC was markedly reduced in both MCT and MCT + VEGFNP/SDFNP groups compared to Ctrl. Since SM-MHC is strictly expressed in mature or fully differentiated vascular smooth muscle cells,[20,21] the decreased expression of this marker indicated a loss of vascular smooth muscle cells in the lung, which is likely associated with peripheral pulmonary vessel pruning as mentioned in the endothelial cell marker expression and discussed above. In contrast, expression of α-SMA was increased in the MCT group, which was significantly reduced by the VEGFNP/SDFNP delivery (Figure 7f). α-SMA is expressed in both mature and immature smooth muscle cells.[22] In response to environmental cues, such as injury, the immature smooth muscle cells exhibit an increased rate of migration and proliferation,[20,22–24] which manifest as muscularization and medial thickening of distal pulmonary vessels in the case of PAH. Thus, the PCR data support the therapeutic effect of VEGFNP/SDFNP. Compared to the histology data shown in Figure 5, however, the measured mRNA level of α-SMA appeared to be underestimated in both the MCT and MCT + VEGFNP/SDFNP groups as the lung section staining showed a significantly higher amount of smooth muscle cells that were present in the distal vessel walls in these groups compared to the control group. This discrepancy is likely due to sampling heterogeneity. PCR measurements were performed using whole lung homogenates, which included both the increased pool of smooth muscle cells in remodeled pulmonary vessel walls and the decreased pool of smooth muscle cells owing to pulmonary vessel pruning.

DISCUSSION

This study examined the effect of VEGFNP/SDFNP in the rat MCT model of PAH. VEGFNPs and SDFNPs were aerosolized into the lungs of the rats at an early- and mid-stage of the disease course to examine the preventive and therapeutic effects in PAH, respectively. The data showed that in both types of the treatments, VEGFNP/SDFNP delivery significantly reduced the pulmonary arterial pressure (measured as RVSP), pulmonary vascular resistance, and thickening of the distal pulmonary vessels. Right ventricular hypertrophy was nearly prevented in the rats, indicating that the VEGFNP/SDFNP treatment had profoundly delayed the progress of PAH development.

The therapeutic effect of VEGFNP/SDFNP was initially thought to be related to the endothelial cell growth function of VEGF. However, gene expression analysis did

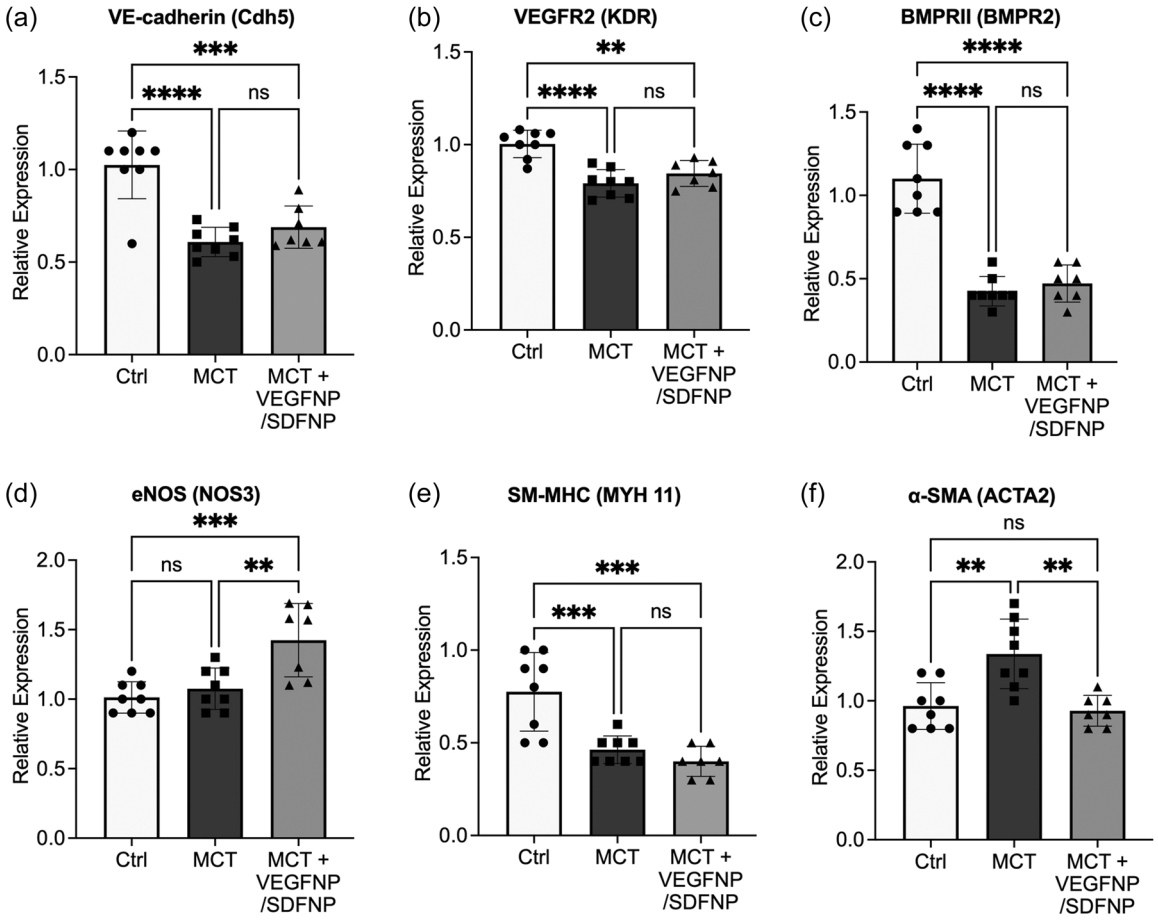

FIGURE 7 Gene expression analysis. RNA was extracted from whole right lung of nude rats, which were treated with nothing (Ctrl), MCT, or MCT + VEGFNP/SDFNP. cDNA quantification was performed with real-time PCR. Protein and gene name are indicated. ns, $p > 0.05$; $^{**}p \leq 0.01$; $^{***}p \leq 0.001$; and $^{****}p \leq 0.0001$. MCT, monocrotaline; NP, nanoparticles; PCR, polymerase chain reaction; SDF, stromal cell-derived factor-1α; VEGF, vascular endothelial growth factor.

not support this assumption. The expression of endothelial cell markers, VE-cadherin, KDR, and BMPR2, in the MCT + VEGFNP/SDFNP treated lungs was comparable to that of MCT lungs, and both were significantly lower than no treatment control. This finding indicates that MCT had caused significant loss of endothelial cells in the rat lungs, which was not restored by the VEGFNP/SDFNP delivery. A previous imaging study has shown that more than half of the distal pulmonary vessels lost branches/junctions in the MCT-treated Sprague Dawley rats.[18] The significant reduction of endothelial cell marker mRNA in the MCT lungs is likely associated with the loss of peripheral/distal capillary vessels. VEGFNP/SDFNP delivery apparently did not facilitate their regrowth. Nevertheless, VEGFNP/SDFNP may have helped in the repair of existing endothelium by replacing apoptotic and dysfunctional endothelial cells. However, the scale of this type of endothelial cell growth would be much less than that lost in the course of peripheral pulmonary vessel pruning, and may not be reflected in the gene expression analysis.

VEGFNP/SDFNP delivery had significantly increased endothelial nitric oxide synthase (eNOS) expression in the MCT lungs. This phenomenon has also been reported in a previous study in which VEGF was delivered to the lungs of rats by adenovirus-mediated gene transfer.[2] VEGF has been known to not only induce eNOS expression [25–27] but also activate eNOS by triggering phosphorylation of the protein at Ser1177.[28–30] eNOS is responsible for the production of nitric oxide (NO) in blood vessels. NO that is released from the endothelium causes underlying smooth muscle relaxation and prevents smooth muscle cell proliferation under pathophysiological conditions.[31,32] This aspect of (improved) endothelial function may explain, at least in part, the observation that VEGFNP/SDFNP delivered to MCT-treated rats was associated with a decrease in muscularization and medial thickening of distal pulmonary vessels.

The present study used CsA-treated Sprague Dawley rats and nude rats to avoid immune elimination of human proteins delivered to the lungs of rats. We

observed that the lungs of the MCT-treated nude rats, were surprisingly clean, with minimal macrophage infiltration. These findings differed from those in MCT-treated Sprague Dawley rat lungs, which often were overwhelmed with macrophages and perivascular inflammation. Since inflammation plays an important role in the development of PAH, lacking this factor may have, in part, accounted for the therapeutic effects of VEGFNP/SDFNP observed in this study. It may also account for the longer time course required to develop PAH in the MCT-injected nude rats compared to that in CsA-treated Sprague Dawley rats (4 vs. 3 weeks, respectively). In future applications, elimination of inflammation might need to be considered to achieve an even better outcome for this treatment.

PAH is a multifactorial disease. Even with the simple model used in this study, multiple mediators in addition to those that we examined may have been involved in the effect of VEGFNP/SDFNP. A systematic analysis may, therefore, help better understand the mechanism underlying the therapeutic effects of this treatment.

AUTHOR CONTRIBUTIONS

Victoria A. Guarino performed experiments, analyzed data, and wrote manuscript. Joseph Loscalzo designed experiments, analyzed and interpreted results, and wrote manuscript. Bradley M. Wertheim performed and analyzed experiments. Wusheng Xiao performed and analyzed experiments. Ying-Yi Zhang designed and performed experiments, analyzed data, interpreted results, and wrote manuscript.

ACKNOWLEDGEMENTS

The authors thank Rose Cannistraro and Stephanie Tribuna for expert assistance in the preparation of this manuscript. The study was supported, in part, by a fund from Astellas Institute for Regenerative Medicine.

CONFLICT OF INTEREST STATEMENT

The authors declare no conflicts of interest.

ETHICS STATEMENT

All animal experiments were approved by the Brigham and Women's Hospital Institutional Animal Care and Use Committee, protocol #s 2016N000332 and 2016N000328.

ORCID

Joseph Loscalzo http://orcid.org/0000-0002-1153-8047

REFERENCES

1. Loscalzo J. Endothelial dysfunction in pulmonary hypertension. N Engl J Med. 1992;327:117–9. https://doi.org/10.1056/NEJM199207093270209
2. Partovian C, Adnot S, Raffestin B, Louzier V, Levame M, Mavier IM, Lemarchand P, Eddahibi S. Adenovirus-mediated lung vascular endothelial growth factor overexpression protects against hypoxic pulmonary hypertension in rats. Am J Respir Cell Mol Biol. 2000;23:762–71. https://doi.org/10.1165/ajrcmb.23.6.4106
3. Taraseviciene-Stewart L, Kasahara Y, Alger L, Hirth P, Mahon GM, Waltenberger J, Voelkel NF, Tuder RM. Inhibition of the VEGF receptor 2 combined with chronic hypoxia causes cell death-dependent pulmonary endothelial cell proliferation and severe pulmonary hypertension. FASEB J. 2001;15:427–38. https://doi.org/10.1096/fj.00-0343com
4. Vitali SH, Hansmann G, Rose C, Fernandez-Gonzalez A, Scheid A, Mitsialis SA, Kourembanas S. The Sugen 5416/hypoxia mouse model of pulmonary hypertension revisited: long-term follow-up. Pulm Circ. 2014;4:619–29. https://doi.org/10.1086/678508
5. Akiyama T, Sadahiro T, Yamada Y, Fujita R, Abe Y, Nakano K, Honda S, Ema M, Kubota Y, Sakai S, Hizawa N, Ieda M. Flk1 deficiency and hypoxia synergistically promote endothelial dysfunction, vascular remodeling, and pulmonary hypertension. Arterioscler Thromb Vasc Biol. 2023;43:1668–83. https://doi.org/10.1161/ATVBAHA.123.319266
6. Winter MP, Sharma S, Altmann J, Seidl V, Panzenböck A, Alimohammadi A, Zelniker T, Redwan B, Nagel F, Santer D, Stieglbauer A, Podesser B, Sibilia M, Helbich T, Prager G, Ilhan-Mutlu A, Preusser M, Lang IM. Interruption of vascular endothelial growth factor receptor 2 signaling induces a proliferative pulmonary vasculopathy and pulmonary hypertension. Basic Res Cardiol. 2020;115:58. https://doi.org/10.1007/s00395-020-0811-5
7. Eyries M, Montani D, Girerd B, Favrolt N, Riou M, Faivre L, Manaud G, Perros F, Gräf S, Morrell NW, Humbert M, Soubrier F. Familial pulmonary arterial hypertension by KDR heterozygous loss of function. Eur Respir J. 2020;55:1902165. https://doi.org/10.1183/13993003.02165-2019
8. Tuder RM, Groves B, Badesch DB, Voelkel NF. Exuberant endothelial cell growth and elements of inflammation are present in plexiform lesions of pulmonary hypertension. Am J Pathol. 1994;144:275–85.
9. Lee SD, Shroyer KR, Markham NE, Cool CD, Voelkel NF, Tuder RM. Monoclonal endothelial cell proliferation is present in primary but not secondary pulmonary hypertension. J Clin Invest. 1998;101:927–34. https://doi.org/10.1172/JCI1910
10. Tuder RM, Radisavljevic Z, Shroyer KR, Polak JM, Voelkel NF. Monoclonal endothelial cells in appetite suppressant-associated pulmonary hypertension. Am J Respir Crit Care Med. 1998;158:1999–2001. https://doi.org/10.1164/ajrccm.158.6.9805002
11. Ceradini DJ, Kulkarni AR, Callaghan MJ, Tepper OM, Bastidas N, Kleinman ME, Capla JM, Galiano RD, Levine JP, Gurtner GC. Progenitor cell trafficking is regulated by hypoxic gradients through HIF-1 induction of SDF-1. Nature Med. 2004;10:858–64. https://doi.org/10.1038/nm1075
12. De Falco E, Porcelli D, Torella AR, Straino S, Iachininoto MG, Orlandi A, Truffa S, Biglioli P, Napolitano M, Capogrossi MC, Pesce M. SDF-1 involvement in endothelial phenotype and ischemia-induced recruitment of bone marrow progenitor cells. Blood. 2004;104:3472–82. https://doi.org/10.1182/blood-2003-12-4423

13. Zampetaki A, Kirton JP, Xu Q. Vascular repair by endothelial progenitor cells. Cardiovasc Res. 2008;78:413–21. https://doi.org/10.1093/cvr/cvn081
14. Berse B, Brown LF, Van de Water L, Dvorak HF, Senger DR. Vascular permeability factor (vascular endothelial growth factor) gene is expressed differentially in normal tissues, macrophages, and tumors. Mol Biol Cell. 1992;3:211–20. https://doi.org/10.1091/mbc.3.2.211
15. Kaner RJ, Ladetto JV, Singh R, Fukuda N, Matthay MA, Crystal RG. Lung overexpression of the vascular endothelial growth factor gene induces pulmonary edema. Am J Respir Cell Mol Biol. 2000;22:657–64. https://doi.org/10.1165/ajrcmb.22.6.3779
16. Guarino VA, Blau A, Alvarenga J, Loscalzo J, Zhang YY. A crosslinked dextran sulfate-chitosan nanoparticle for delivery of therapeutic heparin-binding proteins. Int J Pharm. 2021;610:121287. https://doi.org/10.1016/j.ijpharm.2021.121287
17. Zaman P, Wang J, Blau A, Wang W, Li T, Kohane D, Loscalzo J, Zhang YY. Incorporation of heparin-binding proteins into preformed dextran sulfate-chitosan nanoparticles. Int J Nanomedicine. 2016;11:6149–59. https://doi.org/10.2147/IJN.S119174
18. Zhu Z, Wang Y, Long A, Feng T, Ocampo M, Chen S, Tang H, Guo Q, Minshall R, Makino A, Huang W, Chen J. Pulmonary vessel casting in a rat model of monocrotaline-mediated pulmonary hypertension. Pulm Circ. 2020;10:2045894020922129. https://doi.org/10.1177/2045894020922129
19. Koo HS, Kim KC, Hong YM. Gene expressions of nitric oxide synthase and matrix metalloproteinase-2 in monocrotaline-induced pulmonary hypertension in rats after bosentan treatment. Korean Circ J. 2011;41:83–90. https://doi.org/10.4070/kcj.2011.41.2.83
20. Fukuda D, Aikawa M. Intimal smooth muscle cells: the context-dependent origin. Circulation. 2010;122:2005–8. https://doi.org/10.1161/CIRCULATIONAHA.110.986968
21. Miano JM, Cserjesi P, Ligon KL, Periasamy M, Olson EN. Smooth muscle myosin heavy chain exclusively marks the smooth muscle lineage during mouse embryogenesis. Circ Res. 1994;75:803–12. https://doi.org/10.1161/01.res.75.5.803
22. Owens GK. Regulation of differentiation of vascular smooth muscle cells. Physiol Rev. 1995;75:487–517. https://doi.org/10.1152/physrev.1995.75.3.487
23. Owens GK, Kumar MS, Wamhoff BR. Molecular regulation of vascular smooth muscle cell differentiation in development and disease. Physiol Rev. 2004;84:767–801. https://doi.org/10.1152/physrev.00041.2003
24. Rensen SSM, Doevendans PAFM, van Eys GJJM. Regulation and characteristics of vascular smooth muscle cell phenotypic diversity. Neth Heart J. 2007;15:100–8. https://doi.org/10.1007/BF03085963
25. Bouloumié A. Vascular endothelial growth factor up-regulates nitric oxide synthase expression in endothelial cells. Cardiovasc Res. 1999;41:773–80. https://doi.org/10.1016/s0008-6363(98)00228-4
26. Facemire CS, Nixon AB, Griffiths R, Hurwitz H, Coffman TM. Vascular endothelial growth factor receptor 2 controls blood pressure by regulating nitric oxide synthase expression. Hypertension. 2009;54:652–8. https://doi.org/10.1161/HYPERTENSIONAHA.109.129973
27. Hood JD, Meininger CJ, Ziche M, Granger HJ. VEGF upregulates ecNOS message, protein, and NO production in human endothelial cells. Am J Physiol. 1998;274:1054–8. https://doi.org/10.1152/ajpheart.1998.274.3.H1054
28. Feliers D, Chen X, Akis N, Choudhury GG, Madaio M, Kasinath BS. VEGF regulation of endothelial nitric oxide synthase in glomerular endothelial cells. Kidney Int. 2005;68:1648–59. https://doi.org/10.1111/j.1523-1755.2005.00575.x
29. Gélinas DS, Bernatchez PN, Rollin S, Bazan NG, Sirois MG. Immediate and delayed VEGF-mediated NO synthesis in endothelial cells: role of PI3K, PKC and PLC pathways. Br J Pharmacol. 2002;137:1021–30. https://doi.org/10.1038/sj.bjp.0704956
30. Wang Y, Nagase S, Koyama A. Stimulatory effect of IGF-I and VEGF on eNOS message, protein expression, eNOS phosphorylation and nitric oxide production in rat glomeruli, and the involvement of PI3-K signaling pathway. Nitric oxide. 2004;10:25–35. https://doi.org/10.1016/j.niox.2004.02.001
31. D'Souza FM, Sparks RL, Chen H, Kadowitz PJ, Jeter JR. Mechanism of eNOS gene transfer inhibition of vascular smooth muscle cell proliferation. Am J Physiol-Cell Physiol. 2003;284:C191–9. https://doi.org/10.1152/ajpcell.00179.2002
32. Jeremy J, Rowe D, Emsley AM, Newby AC. Nitric oxide and the proliferation of vascular smooth muscle cells. Cardiovasc Res. 1999;43:580–94. https://doi.org/10.1016/s0008-6363(99)00171-6

How to cite this article: Guarino VA, Wertheim BM, Xiao W, Loscalzo J, Zhang Y-Y. Nanoparticle delivery of VEGF and SDF-1α as an approach for treatment of pulmonary arterial hypertension. Pulm Circ. 2024;14:e12412. https://doi.org/10.1002/pul2.12412